PHYSICAL REVIEW B **82**, 100411(R) (2010)

Spontaneous formation of an exchange-spring composite via magnetic phase separation in $Pr_{1-x}Ca_xCoO_3$

S. El-Khatib,[1,2,3] Shameek Bose,[1] C. He,[1] J. Kuplic,[1] M. Laver,[2,3,*] J. A. Borchers,[2] Q. Huang,[2] J. W. Lynn,[2] J. F. Mitchell,[4] and C. Leighton[1,†]

[1]*Department of Chemical Engineering and Materials Science, University of Minnesota, Minneapolis, Minnesota 55455, USA*

[2]*NIST Center for Neutron Research, National Institute of Standards and Technology, Gaithersburg, Maryland 20899, USA*

[3]*Department of Materials Science and Engineering, University of Maryland, College Park, Maryland 20742, USA*

[4]*Materials Science Division, Argonne National Laboratory, Argonne, Illinois 60439, USA*

(Received 12 July 2010; revised manuscript received 9 August 2010; published 22 September 2010)

We present a neutron-diffraction, small-angle scattering, and magnetometry study of the narrow bandwidth perovskite cobaltite $Pr_{1-x}Ca_xCoO_3$, demonstrating an unusual form of magnetoelectronic phase separation where long-range ordered ferromagnetism coexists spatially with short-range ferromagnetism. The two phases have very different coercivities and, remarkably, are strongly exchange coupled. The electronic phase separation thus leads to spontaneous formation of a hard-soft nanocomposite, exhibiting prototypical exchange-spring behavior in the absence of chemical interfaces.

DOI: 10.1103/PhysRevB.82.100411 PACS number(s): 75.25.−j, 75.47.Lx, 75.60.Jk

After several years of intensive studies of complex oxides such as manganites and cuprates, it is now clear that competing interactions in these correlated systems lead to a delicate competition between ground states.[1–3] This has many interesting consequences, including colossal response to applied fields,[1–3] stabilization of new states at interfaces (e.g., Refs. 4 and 5), and an instability toward magnetoelectronic phase separation.[1–3] The latter effect, where multiple electronic/magnetic phases coexist spatially, in the absence of gross chemical segregation, is now well established[1–3] and is supported by several models.[3,6,7] Detailed work has elucidated several complex phenomena, including preformation of clusters above long-range-ordering (LRO) temperatures,[3,8] field- and temperature-dependent phase competition,[3,9,10] and electronic inhomogeneity over a range of length scales[3,8–12] and morphologies.[3,8–15]

One aspect of the behavior of electronically phase-separated oxides that remains unclear is the issue of *coupling* between phase-separated regions. Spatial coexistence has been observed for a variety of local orders [e.g., ferromagnetic (FM), antiferromagnetic (AF), and charge/orbitally ordered],[1–3,8–15] but evidence of coupling between them is scarce. In magnetic systems clear signatures exist for exchange coupling between common forms of order, e.g. exchange bias at AF/FM interfaces[16] and exchange-spring behavior at hard/soft FM interfaces.[17] Nevertheless, exchange bias is observed only sporadically in bulk electronically phase separated oxides (it is often ascribed to complex glassy interactions [e.g., Refs. 18 and 19] rather than direct AF/FM coupling[20,21]) while intrinsic exchange-spring magnetism remains elusive. It is unclear why these observations are scarce and under what conditions strong exchange coupling can be established between coexisting phases. Here, we study a perovskite cobaltite, $Pr_{1-x}Ca_xCoO_3$, using smaller ionic radius to suppress LROFM and promote phase competition. We find that a weak LROFM phase coexists with short-range-ordered (SRO) FM, the two phases possessing different coercivities. This unusual form of magnetic phase separation thus leads to formation of a hard/soft FM composite, exhibiting classic exchange-spring behavior, analogous to artificial systems. These results provide evidence of coupling between coexisting FM regions (thus generating exchange-spring magnetism), create a potential means to probe the spin structure of the interface region, and underscore the ability of electronic phase separation to produce nanostructured properties without chemical interfaces.

Polycrystalline $Pr_{1-x}Ca_xCoO_{3-d}$ $(0.00 \leq x \leq 0.40)$ was synthesized from Pr_6O_{11}, $CoC_2O_4 \cdot 2H_2O$, and $CaCO_3$ by solid-state reaction in flowing O_2 at 1000 °C, followed by cold pressing, sintering (1200 °C in O_2), and slow cooling (0.5 °C/min). Rietveld refinement of neutron powder diffraction (NPD) indicated single-phase material in the *Pnma* space group (as in Refs. 22 and 23) while scanning transmission electron microscopy revealed no indication of secondary phase clusters. Thermogravimetric analysis revealed small O deficiency to $x=0.30-0.40$ ($\delta=0.04$), beyond which it increases quickly. Measurements are thus restricted to $x \leq 0.40$. NPD and small-angle neutron scattering (SANS) were performed at the NIST Center for Neutron Research (BT-1, BT-9, and NG7), at wavelengths of 1.54 Å and 5.00 Å, respectively. Figure 1 shows a magnetic phase diagram (from NPD, SANS, transport, magnetometry, and heat capacity that will be published elsewhere), to provide a glo-

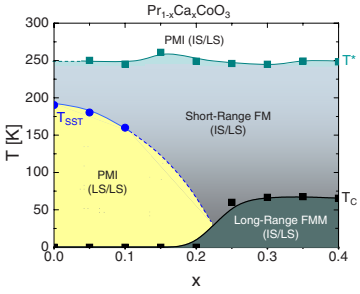

FIG. 1. (Color online) Magnetic phase diagram of $Pr_{1-x}Ca_xCoO_3$. T_{SST}, T_C, and T^* are the onset spin-state transition temperature, Curie temperature, and temperature at which short-range ferromagnetism occurs. PMI is paramagnetic insulator and FMM is ferromagnetic metal. The fields are labeled with the spin state of the (Co^{3+}/Co^{4+}) ions.

bal picture of the magnetic properties. These are rather different than $La_{1-x}Sr_xCoO_3$ (LSCO),[24] due to the smaller *A*-site cations. This results in (a) increased deviations from 180° Co-O-Co bond angle, (b) a reduction in tolerance factor, which is expected to suppress FM, and (c) increased stability of low-spin (LS) Co^{3+} due to the larger spin gap arising from the narrower e_g-derived band.[25] This results in two unique situations. First, suppression of FM order promotes competition with competing ground states, enhancing phase separation. Second, we are provided with an opportunity to study the interplay between phase separation and spin state. These features are clearly visible in Fig. 1. At $x=0$ the *onset* temperature of the spin-state transition (T_{SST}) is almost 200 K,[25,26] increased from 30 K in LSCO. $T_{SST}(x)$ marks the transition from an LS/LS state for Co^{3+}/Co^{4+} to a state with finite spin Co^{3+}. Based on prior work, intermediate spin (IS)/LS is expected.[22] As x is increased, T_{SST} decreases due to stabilization of IS Co^{3+}, although above 0.10 the signature of T_{SST} is obscured by paramagnetic Co^{4+}.[27] Remarkably, but in agreement with recent work,[22] between $x=0.20$ and 0.25 a LROFM state abruptly appears. Given this, we speculate that T_{SST} extrapolates to zero at this x (dotted line), i.e., FM occurs as soon as finite spin Co^{3+} ions are stabilized to sufficiently low T. Note that T_C ($\approx$70 K) is suppressed compared to LSCO ($T_C=230$ K at $x=0.3$).[24] At higher T, we find clear evidence of a temperature scale, T^* ($\approx$250 K), where short-range FM spin correlations begin. Below, we will focus on a single x representative of the FM phase (0.30), illustrating the behavior in detail.

The T dependence of the magnetization, M [measured in a field, $\mu_0 H=1$ mT after field cooling (FC) and zero FC (ZFC)] is shown in Fig. 2(d). A sharp increase in the FC $M(T)$ is observed at 70 K, along with an increase in remnance [M_R, Fig. 2(e)]. NPD confirms FM,[23] with $T_C \approx 70$ K. Figure 2(a) shows the T dependence of the resolution limited FM (101) reflection, confirming LRO. Hysteresis loops at 10 K [Fig. 3(a)] have a large high H slope and an FM magnetization, M_S, of only 0.2 μ_B/Co, suggesting that, although the FM is LRO, its volume fraction is <1, i.e., the material is not in a single LROFM phase. Crude estimates based on comparison to the expected M_S suggest volume fractions $\sim$10%. Additional evidence for multiple magnetic phases is provided below. Figure 2(d) also shows a tail in the FC $M(T)$ well above 70 K, which joins the ZFC curve at 250 K (see inset). As shown in Fig. 2(e), this is accompanied by finite M_R and coercivity (H_C), which disappear at 250 K. The origin of this high-T magnetism is clarified by the magnetic SANS cross section, $d\Sigma/d\Omega(T)$, which is plotted in Fig. 2(b) at $q=0.005$ Å^{-1} (a length scale of $\sim$1000 Å) and $q=0.08$ Å^{-1} (tens of angstrom). The low-q $d\Sigma/d\Omega$ turns on at 70 K, consistent with the LROFM [Figs 2(a), 2(d), and 2(e)]. At such low q, $d\Sigma/d\Omega(q)$ adheres to the Porod law, $d\Sigma/d\Omega \propto q^{-4}$ (due to scattering from LROFM domains), as discussed in detail in Ref. 28. The high-q $d\Sigma/d\Omega$ [Fig. 2(b)] is distinctly different from the critical scattering behavior in conventional single-phase LROFM systems. First, it exhibits a long high-T tail, to temperatures far in excess of T_C. The high-T region is magnified in the inset, to illustrate the similarity to $M(T)$ [inset to Fig. 2(d)]. This indicates that short-range spin correlations begin at a well-defined temperature,

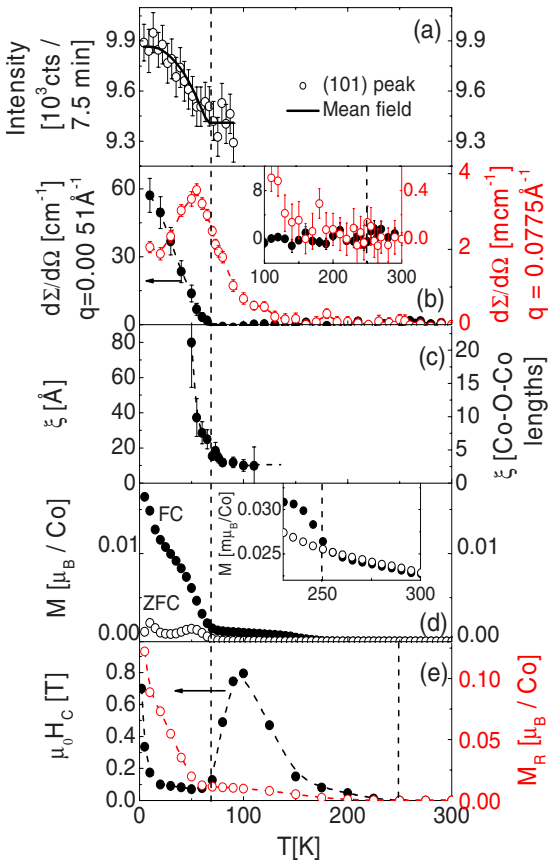

FIG. 2. (Color online) Temperature dependence (at $x=0.30$) of (a) the intensity of the (101) neutron-diffraction peak, (b) the magnetic small-angle neutron scattering absolute cross section at high q (0.078 Å^{-1}, right axis, after subtraction of the Porod component) and low q (0.005 Å^{-1}, left axis), (c) the magnetic correlation length, (d) the 1 mT magnetization after field cooling and zero field cooling, and (e) the coercivity (left axis) and remnant magnetization (right axis). In (b) and (e) the insets are closeups around 250 K. Dotted lines are guide to the eyes; the solid line in (a) is a mean-field order parameter. Vertical dotted lines mark T_C and T^*. Error bars are based on one standard deviation.

T^*. Given that these correlations are accompanied by enhanced M, and finite M_R and H_C, we identify them as FM. At lower T we observe a peak in the high-q $d\Sigma/d\Omega(T)$ (not at T_C) but $d\Sigma/d\Omega$ does *not* fall to zero as T is further lowered. This is in sharp contrast to a fully long-range ordered FM, demonstrating that this system does not exhibit phase pure LROFM. There is in fact a wide range, below 70 K, where LROFM and SROFM spin correlations occur simultaneously. In the high-q range, $d\Sigma/d\Omega(q)$ is Lorentzian (see Ref. 28), providing a magnetic correlation length, ξ, of around 10 Å at $T>70$ K (independent of T), increasing to $\sim$80 Å at lower T [Fig. 2(c)].[28] Above 110 K the scattering is too weak to extract ξ.

We interpret the data of Fig. 2 within a picture illustrated in Fig. 3(c). At T^*, FM spin correlations emerge with a correlation length of 2–3 Co-O-Co lengths, accompanied by finite M_R and H_C. Given this short range, we believe that small spin clusters, or polarons, are responsible.[29] In LSCO there is accumulating evidence for seven-site spin-state polarons,

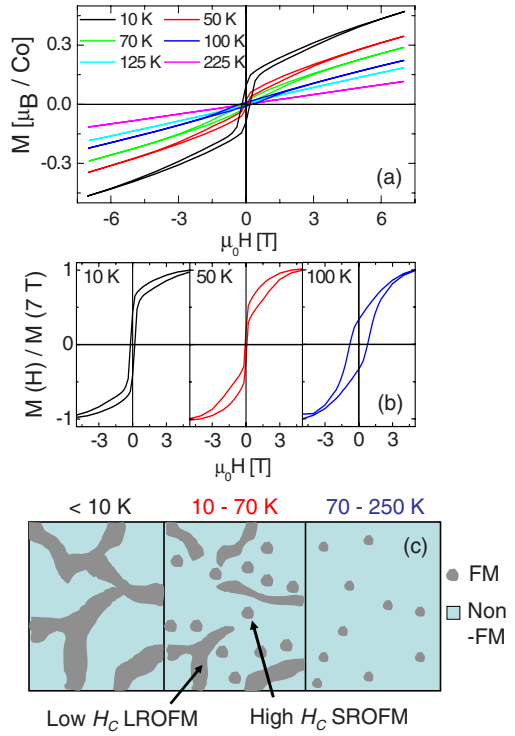

FIG. 3. (Color online) (a) Hysteresis loops at 10–225 K (top to bottom in the first quadrant). (b) Normalized and high-field slope subtracted hysteresis loops at 10, 50, and 100 K. (c) Schematic illustration of the three temperature regimes. Data are for $x=0.30$.

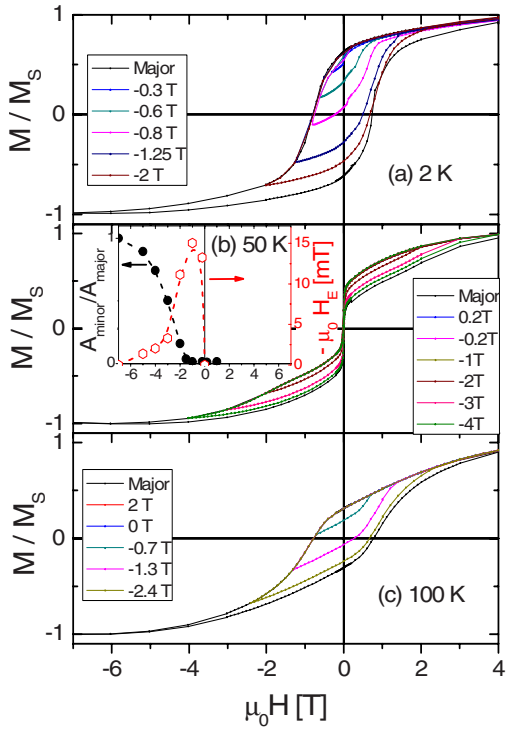

FIG. 4. (Color online) Normalized and high-field slope subtracted hysteresis loops (both major and minor) at (a) 2 K, (b) 50 K, and (c) 100 K. The minor loops were initiated at +7 T and labeled with the final field of the sweep. Inset to (b): 50 K field dependence of the area of the minor loop normalized to the area of the major loop (left axis) and the exchange shift of the minor loop (right axis).

where a Co^{4+} ion stabilizes six nearest-neighbor IS Co^{3+} ions, the doped hole being delocalized within the cluster.[30–32] The expected spatial extent of such a polaron (two Co-O-Co lengths in the absence of any interpolaron correlations) is quite consistent with our data (2.6 Co-O-Co distances at the highest T), although the spin excitons believed to form around O defects in LCO are also possible.[33] As T is lowered the cluster density increases down to 70 K, at which point longer range FM clusters emerge and form a network, providing the LROFM detected by NPD and SANS. As in LSCO, it is likely that the nucleation of this network is influenced by local doping fluctuations.[34] Due to the suppressed FM exchange the volume fraction of the LROFM phase is low, resulting in a state below 70 K [Fig. 3(c)] where an LROFM network exists within a non-FM matrix containing SRO clusters/polarons. The situation is analogous to LSCO at intermediate x (i.e., 0.17–0.22), where a LROFM network of coalesced clusters coexists with a non-FM matrix exhibiting incommensurate magnetism ascribed to spin-state polarons.[31] At still lower T the LROFM phase fraction grows at the expense of the SROFM phase and the high-q $d\Sigma/d\Omega$ drops. As discussed below, $M(H)$ loops at sufficiently low T (2 K) are dominated by the LROFM phase.

The most interesting behavior is shown in Figs. 2(e), 3(a), and 3(b). As touched upon above, close inspection of $M(H)$ at $T>70$ K reveals significant H_C. Figure 2(e) shows that H_C turns on at 250 K, increasing with decreasing T to about 0.8 T at 100 K. The finite M_R and H_C indicate that the SROFM clusters/polarons possess magnetocrystalline anisotropy (MCA). Although this is perhaps surprising, note that (a) the range of the spin correlations, though short, *is* sufficient to sample the crystal structure and (b) spin excitons in LCO are thought to acquire finite M_R via interaction with the matrix.[33] Remarkably, as T is further lowered, and the LROFM phase orders, H_C falls by an order of magnitude in a T interval of only 50 K. As T is further reduced, deep into the LROFM phase, H_C increases again, reflecting the thermally activated nature of the reversal. It is clear from these data that the LROFM phase has considerably lower H_C than the high-T SRO regions. This could reflect a weaker MCA (possible, given the importance of the surface for small clusters/polarons) or reduced H_C due to domain formation in the LROFM network. The latter is analogous to the single domain to multidomain crossover in FM nanoparticles and the percolation-induced H_C reduction in FMs.[24]

The highly unusual region from 50 to 100 K, where $dH_C/dT>0$, is reminiscent of thermal exchange-spring behavior in coupled hard/soft systems with distinct T_C's,[35] where the ordering of the lower H_C low-T phase lowers the overall H_C via exchange coupling to the high-H_C phase. $M(H)$ loops where the high-H slope has been subtracted and M is normalized to its high-H value [Fig. 3(b)], add weight to this argument. At both 10 K (the LROFM region) and 100 K (the SROFM region) we find relatively featureless loops, albeit with rather different H_C and M_R/M_S. At intermediate T (i.e., 50 K), $M(H)$ is very different, exhibiting the characteristic "split-loop" appearance of hard/soft composites. A rapid reversal occurs at low H, followed by a gradual response to

high negative H. Minor loops [Fig. 4(b)] were obtained by applying +7 T, reducing H to a series of values from +1 down to −7 T, then sweeping back to +7 T. Remarkably, there exists a large region over which $M(H)$ is completely reversible. In fact, H can be reduced to values as low as −2 T [Fig. 4(b)] before the recoil $M(H)$ deviates from the major loop. At field values <-2 T, the minor loops open, indicating an abrupt onset of irreversibility. This is clearer in the inset, where the normalized minor loop area (A_{minor}/A_{major}) is negligible down to −2 T, above which it increases rapidly. This is prototypical exchange-spring behavior.[17] The reversibility arises from field-induced winding of an exchange spring in the relatively large soft regions [i.e., the LROFM cluster network in Fig. 3(c)], leaving the spins at the magnetic interface pinned by exchange coupling to the hard region (the SROFM clusters/polarons). In essence, a partial domain wall forms in the soft regions, being compressed toward the interface as H is decreased. As H is increased back to +7 T, the recoil is highly reversible due to unwinding of the exchange spring. If H decreases beyond −1.5 T however, the spring "breaks" and reversal of the hard regions occurs, leading to strong irreversibility [Fig. 4(b)]. This is completely absent in minor loops at 2 and 100 K [Figs. 4(a) and 4(c)], where the hard/soft coexistence no longer occurs. These loops reveal strong irreversibility at all H, i.e., conventional coercive mechanisms. Although the above provides unequivocal evidence for exchange coupling between phase-separated regions, the *mechanism* for the coupling is far from clear. The reversal of the soft regions at $H<0$ indicates that this is predominantly FM (AF interactions lead to reversal at $H>0$) while the observation of such clear exchange-spring behavior indicates that the coupling must be of significant strength. This is quantified by the data on the right axis of the inset of Fig. 4(b), which show the exchange shift (H_E, the displacement of the minor loop from zero field) vs minor loop final field. H_E is negative, shows a significant maximum value of 15 mT, then decreases rapidly as the irreversibility field of the hard loop is exceeded, as expected for a coupled hard-soft system. Development of a reasonable understanding of the *mechanisms* by which the LROFM cluster network can couple to the SRO clusters/polarons, hinges on an understanding of the interaction with the non-FM matrix however, which is in its infancy.[33]

In summary, we have shown that $Pr_{1-x}Ca_xCoO_3$ exhibits an unusual form of magnetic phase separation where short-range ferromagnetic order coexists with long-range ferromagnetism. This leads to the observation of spontaneous formation of a hard/soft composite displaying prototypical exchange-spring magnetism, a rare example of strong coupling between magnetically phase-separated regions in a complex oxide. In addition to providing a potential means to improve our understanding of the interface region between coexisting phases, these results highlight the ability of electronic phase separation to access nanostructured magnetism, in the absence of chemical interfaces.

Work at UMN supported by DOE (Grant No. DE-FG02-06ER46275, neutron scattering) and NSF (Grant No. DMR-0804432). Work at ANL supported by DOE (Grant No. DE-AC02-06CH11357).

*Present address: Paul Scherrer Institut, Villigen, Switzerland.
†Corresponding author; leighton@umn.edu

[1] Y. Tokura and Y. Tomioka, J. Magn. Magn. Mater. **200**, 1 (1999).
[2] J. M. D. Coey *et al.*, Adv. Phys. **48**, 167 (1999).
[3] E. Dagotto, *Nanoscale Phase Separation and Colossal Magnetoresistance* (Springer, New York, 2002); E. Dagotto *et al.*, Phys. Rep. **344**, 1 (2001); E. Dagotto, Science **309**, 257 (2005).
[4] A. Ohtomo and H. Y. Hwang, Nature (London) **427**, 423 (2004).
[5] S. Smadici *et al.*, Phys. Rev. Lett. **99**, 196404 (2007).
[6] K. I. Kugel *et al.*, Phys. Rev. Lett. **95**, 267210 (2005).
[7] K. H. Ahn *et al.*, Nature (London) **428**, 401 (2004).
[8] J. M. de Teresa *et al.*, Nature (London) **386**, 256 (1997).
[9] P. Dai *et al.*, Phys. Rev. Lett. **85**, 2553 (2000).
[10] G. R. Blake *et al.*, Phys. Rev. B **66**, 144412 (2002).
[11] M. Uehara *et al.*, Nature (London) **399**, 560 (1999).
[12] E. Granado *et al.*, Phys. Rev. B **68**, 134440 (2003).
[13] J. Tao *et al.*, Phys. Rev. Lett. **94**, 147206 (2005).
[14] Ch. Simon *et al.*, Phys. Rev. Lett. **89**, 207202 (2002).
[15] M. Viret *et al.*, Phys. Rev. Lett. **93**, 217402 (2004).
[16] J. Nogués and I. K. Schuller, J. Magn. Magn. Mater. **192**, 203 (1999); A. E. Berkowitz and K. Takano, *ibid.* **200**, 552 (1999).
[17] E. E. Fullerton *et al.*, J. Magn. Magn. Mater. **200**, 392 (1999).
[18] Y.-K. Tang *et al.*, J. Appl. Phys. **100**, 023914 (2006); Y. K. Tang *et al.*, Phys. Rev. B **73**, 174419 (2006).
[19] S. Karmakar *et al.*, Phys. Rev. B **77**, 144409 (2008).
[20] D. Niebieskikwiat and M. B. Salamon, Phys. Rev. B **72**, 174422 (2005).
[21] T. Qian *et al.*, Appl. Phys. Lett. **90**, 012503 (2007).
[22] S. Tsubouchi *et al.*, Phys. Rev. B **69**, 144406 (2004); S. Tsubouchi *et al.*, *ibid.* **66**, 052418 (2002).
[23] A. Chichev *et al.*, J. Magn. Magn. Mater. **316**, e728 (2007); A. Chichev *et al.*, Z. Kristallogr. **26**, 435 (2007).
[24] J. Wu and C. Leighton, Phys. Rev. B **67**, 174408 (2003); H. M. Aarbogh *et al.*, *ibid.* **74**, 134408 (2006).
[25] M. Tachibana *et al.*, Phys. Rev. B **77**, 094402 (2008).
[26] J.-Q. Yan *et al.*, Phys. Rev. B **69**, 134409 (2004).
[27] The Pr paramagnetic signal was also subtracted from the data, following Ref. 26.
[28] See supplementary material at http://link.aps.org/supplemental/10.1103/PhysRevB.82.100411 for more detailed information on $d\Sigma/d\Omega(q)$ and Porod/Lorentzian fits.
[29] We use the correlation length extracted in this manner as an estimate of the magnetic cluster size, even though this is not strictly applicable to finite-size magnetic entities.
[30] S. Yamaguchi *et al.*, Phys. Rev. B **53**, R2926 (1996).
[31] D. Phelan *et al.*, Phys. Rev. Lett. **97**, 235501 (2006).
[32] A. Podlesnyak *et al.*, Phys. Rev. Lett. **101**, 247603 (2008).
[33] S. R. Giblin *et al.*, Europhys. Lett. **70**, 677 (2005); S. R. Giblin *et al.*, Phys. Rev. B **74**, 104411 (2006); S. R. Giblin *et al.*, *ibid.* **79**, 174410 (2009).
[34] C. He *et al.*, EPL **87**, 27006 (2009).
[35] This is similar to heterostructures such as FeRh/FePt, J.-U. Thiele *et al.*, Appl. Phys. Lett. **82**, 2859 (2003).